

# Machine Learning in the Problem of No-Core Shell Model Result Extrapolations

R. E. Sharypov<sup>1</sup>, A. I. Mazur<sup>1\*</sup>, and A. M. Shirokov<sup>2</sup>

<sup>1</sup>*Pacific National University, Khabarovsk, 680035 Russia*

<sup>2</sup>*Skobeltsyn Institute of Nuclear Physics, Moscow State University, Moscow, 119991 Russia*

Received October 9, 2024; revised October 17, 2024; accepted October 17, 2024

**Abstract**—A method for extrapolating the results of variational calculations to the case of the infinite basis using an ensemble of artificial neural networks is proposed. Extrapolations of the no-core shell model results obtained with the nucleon–nucleon interaction Daejeon16 for the ground state energies, as well as for the root-mean-square (rms) point-proton, point-neutron, and point-nucleon (matter) radii of the <sup>6</sup>Li and <sup>6</sup>He nuclei, are performed.

**DOI:** 10.1134/S1063778824700868

## 1. INTRODUCTION

In recent years, neural network machine learning methods have become a part of the arsenal of theoreticians and experimentalists in the field of nuclear physics (see review [1]). A special class of problems in this field, which has not been fully explored and requires the development of new algorithms, is the extrapolation of the results of variational calculations to the case of the infinite basis.

Modern studies of the properties of light nuclei are carried out in *ab initio* (first principles) approaches using realistic nucleon–nucleon (*NN*) forces. One such approach is the no-core shell model (NCSM) [2], in which all nucleons of the nucleus are spectroscopically active. The parameters of the many-body oscillator basis of the NCSM are the number of oscillator excitation quanta  $N_{\max}$  taken into account, which determines the size of the model space, and the oscillator energy  $\hbar\Omega$ .

Models of realistic *NN* interactions have long been constructed within the meson exchange theory. Currently, *NN* potentials constructed within the chiral effective field theory are used more often. A detailed review of modern models of nucleon–nucleon forces is given in [3]. Realistic *NN* potentials reproduce nucleon–nucleon scattering data and deuteron properties with high accuracy. Three-nucleon forces are additionally taken into account when studying nuclei.

The number of NCSM basis functions grows exponentially with increasing  $N_{\max}$ , which leads to a sharp increase in the required computing resources. Modern supercomputers allow calculations in NCSM to be carried out with reasonable accuracy for light nuclei with a mass number up to  $A \simeq 20$ ; moreover, while for the lightest *s*-shell and the beginning of the *p*-shell nuclei (<sup>3</sup>He, <sup>3</sup>H, <sup>4</sup>He, <sup>6</sup>He, <sup>6</sup>Li) calculations with  $N_{\max} \simeq 20$  are possible, for the nuclei in the middle of the *p*-shell the calculations are available only with  $N_{\max} \leq 14$ . As a result, the NCSM calculations of observed atomic nuclei typically fail to achieve full convergence.

To predict converged results corresponding to the infinite basis, various phenomenological extrapolation methods have been proposed [4–12]. The method [13] in which the extrapolation results are determined by localizing the poles of the *S* matrix for bound states seems to be the most justified one.

Another interesting possibility of using machine learning methods for extrapolating variational calculations to the case of the infinite basis was proposed in [14]. Subsequently, works [15–18] were published where other approaches to extrapolating NCSM results using machine learning were considered.

In continuation of the study [14], to obtain final predictions, we proposed [19] to use a more complex topology of the artificial neural network and formulated strict criteria for the selection of trained networks. As a result, there is no need to divide all the data used into training and test sets in our approach: all data are used for training, since our approach has

---

\*E-mail: amazur.pnu.khb@mail.ru

no problem of overfitting. This is very important, since it allows us to significantly increase the statistical reliability of our predictions by taking into account the selection of trained networks on the basis of the formulated criteria.

The aim of this work is to continue research in this direction. We apply the method of training an ensemble of neural networks and selecting trained networks developed in [19] to the problem of extrapolating the energies and root-mean-square (rms) radii of the distributions of point protons  $r_p$ , point neutrons  $r_n$ , and point nucleons (matter)  $r_m$  in the ground states of  ${}^6\text{He}$  and  ${}^6\text{Li}$  nuclei on the basis of NCSM calculations with the  $NN$  interaction Daejeon16 [20], constructed within the chiral effective field theory. The off-shell properties of this potential are determined by fitting to the properties of light nuclei using phase-equivalent transformations, which allows description of nuclei without using three-nucleon forces.

In [14], the extrapolations of the energy and rms radius  $r_p$  of the ground state of the  ${}^6\text{Li}$  nucleus was carried out using machine learning methods on the basis of the same NCSM results. Of interest is also a comparison with the results of the two-dimensional phenomenological extrapolation of the rms radii  $r_p$ ,  $r_n$ , and  $r_m$  of the ground states of the  ${}^6\text{He}$  and  ${}^6\text{Li}$  nuclei based also on the NCSM calculations with the Daejeon16 potential [12, 21].

## 2. BRIEF DESCRIPTION OF THE METHOD. NEURAL NETWORK TOPOLOGY

The neural network used in this work is a multi-layer perceptron with three hidden layers. The input layer contains two neurons, the output layer contains one neuron, and each of the hidden layers contains ten neurons. This neural network has been tested on the problem of extrapolating results of variational calculations of the ground state energy of atomic nuclei with different  $NN$  potentials [19]. The topology of the neural network is shown in Fig. 1.

The action of our neural network can be described by the formula

$$y = l_4 (W_{43} \circ \sigma_3 (W_{32} \circ \sigma_2 (W_{21} \circ l_1 (W_{10} \circ \mathbf{x}))), \quad (1)$$

where  $\mathbf{x}$  are the values of  $N_{\max}$  and  $\hbar\Omega$  of neurons of the input layer, and  $y$  takes the values of  $E$ , or  $r_p$ , or  $r_n$ , or  $r_m$  from the training set. The action of the operator  $W_{pq}$  is as follows: each neuron  $x_p^i$  of the layer  $p$  collects all input signals  $x_q^j$  of the previous layer  $q$  and calculates their weighted sum:

$$x_p^i = \sum_j \omega_{pq}^{ij} \cdot x_q^j + b_p^i. \quad (2)$$

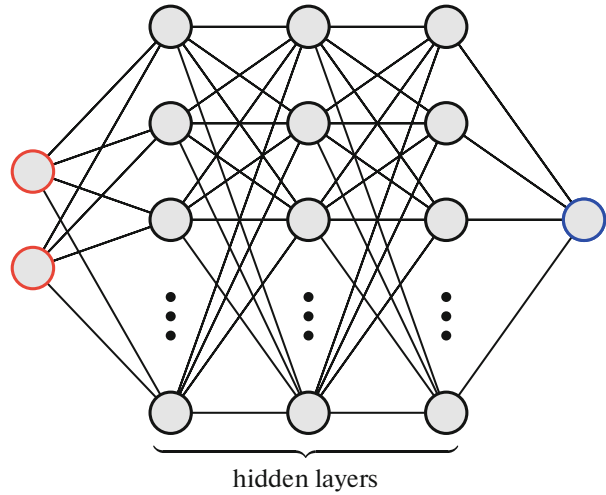


Fig. 1. Neural network topology.

The obtained signal  $x_p^i$  is transformed by the activating function  $f_p(x_p^i)$  and is transmitted to all neurons of the next layer. Weights  $\omega_{pq}^{ij}$  and biases  $b_p^i$  are the trainable parameters of the neural network. Training the neural network consists in fitting the trainable parameters in such a way as to minimize the loss function: in our case, the mean square deviation of the neural network predictions from the training dataset.

In our network, the linear activating function  $f_p(x) \equiv l(x) = x$  ( $p = 1, 4$ ) is used in the first hidden and in the output layer, and the sigmoid function  $f_p(x) \equiv \sigma(x) = 1/(1 + \exp(-x))$  is used in the other layers ( $p = 2, 3$ ). Training is performed by the gradient descent method using the Adam algorithm [22]. The total number of trainable parameters for the topology presented in Fig. 1 is 261.

It is important to note that the initialization of the training parameters for each network ensemble of the model occurs randomly. As a result, when retraining on the same training dataset, the loss function falls into a different local minimum, and the result of the neural network prediction differs. In order to obtain reliable predictions, an ensemble of neural networks is trained (in our case, 1024 neural networks). That is, the extrapolation method consists in training an ensemble of neural networks on a set of NCSM calculations of a particular observable of an atomic nucleus, carried out with different values of the oscillator parameter  $\hbar\Omega$  in model spaces  $N_{\max}$  up to  $N_{\max}^u$ . The input data of the neural network are the NCSM parameters  $N_{\max}$  and  $\hbar\Omega$ , and the output data are the corresponding observable values obtained in the NCSM. The set of these data,  $N_{\max}$ ,  $\hbar\Omega$ , and  $E$  (or  $r_p$ , or  $r_n$ , or  $r_m$ ), form a training set. Using the

trained neural networks, the observables are calculated in higher model spaces up to a certain maximum value of  $N_{\max}^f$  at which convergence is assumed to be achieved.

The trained neural networks are next selected according to the criteria discussed below. The predicted value and the uncertainty of extrapolation of the observable are determined as a result of statistical processing of the distribution of predictions of selected neural networks. A more detailed description of the method is given in [19].

### 3. INITIAL DATA AND THEIR PREPROCESSING

Figures 2a, 2b and 3a, 3b show the results of NCSM calculations with  $NN$  interaction Daejeon16 of the ground state energies and rms radii of  ${}^6\text{He}$  and  ${}^6\text{Li}$  nuclei. It was shown in [13] that stable extrapolation results by the SS-HORSE–NCSM method are achieved only when using data lying to the right of the minimum of the energy dependence on  $\hbar\Omega$  in each model space. The experience with numerical calculations has shown that such data selection significantly improves the energy extrapolation using machine learning as well [19]. Therefore, data in the ranges of the oscillator parameter from the variational minimum for each model space up to  $\hbar\Omega = 40$  MeV are included the training set in the energy extrapolation problem. To study the convergence of the method, we expanded the number of training data by successively increasing  $N_{\max}^u$  and utilizing the NCSM results from model spaces from  $N_{\max} = 4$  to  $N_{\max}^u$ .

In problems of extrapolation of rms point radii  $r_m$ ,  $r_n$ , and  $r_p$ , we included data from the range  $12.5 \leq \hbar\Omega \leq 40$  MeV in the training set. Before training the neural network, all quantities of the training set— $N_{\max}$ ,  $\hbar\Omega$ , and  $E$  (or  $r_p$ , or  $r_n$ , or  $r_m$ )—are scaled linearly to equal intervals  $[0, 1]$ .

### 4. CRITERIA FOR SELECTION OF TRAINED NEURAL NETWORKS AND STATISTICAL PROCESSING OF RESULTS

As already noted, the loss function for each neural network from the ensemble falls into its local minimum because of the random initialization of the training parameters and the stochastic nature of the training process. Therefore, the predictions obtained using the neural networks ensemble differ and are described by a certain distribution, and require statistical processing.

Not all trained networks produce reasonable results, so it is necessary to perform a selection before statistical processing. For the problem of the ground state extrapolation, we formulated and used the following criteria [19]:

- “Soft variational principle”: energy predictions for consecutive  $N_{\max}$  should satisfy the variational principle with the allowance for its small violation due to numerical errors by no more than 0.1 keV for predictions in neighboring model spaces.
- “Convergence criterion,” which is as follows. First, model spaces  $N_{\max}^c$  ( $N_{\max}^u < N_{\max}^c < N_{\max}^f$ ) are found that simultaneously satisfy two conditions: 1) the condition of weak dependence of the ground state energy on the oscillator parameter  $\hbar\Omega$  (the difference between the maximum and minimum energy values in the model space  $N_{\max}^c$  should not exceed  $\varepsilon_1 = 0.02$  MeV), and 2) the difference between the minimum energy values in adjacent spaces  $N_{\max}^c$  and  $N_{\max}^c + 2$  should not exceed  $\varepsilon_2 = 0.001$  MeV. Then 80% of the fastest converging networks are selected from the obtained distribution of neural networks over  $N_{\max}^c$ .
- “Straightness criterion”: the requirement of a weak dependence of the predictions of the observable on the oscillator parameter  $\hbar\Omega$  in a given interval for  $N_{\max} = N_{\max}^f$ . We use  $\varepsilon_s = 0.002$  MeV as the permissible deviation due to numerical errors for the difference between the maximum and minimum values of the extrapolated energies in the selected interval  $\hbar\Omega$ .

Only the last criterion is used in problems of the extrapolation of rms point radii, we use  $\varepsilon_r = 0.002$  fm for the difference between the maximum and minimum values of the extrapolated radii.

The neural network is discarded and does not participate in further statistical processing if at least one of the criteria is not met.

In addition, to exclude obvious outliers in the training quality, we discarded 5% of neural networks with the highest loss function values at the end of training, i.e., after the selection according to the specified criteria.

A prediction is calculated for a sufficiently larger  $N_{\max} = N_{\max}^f$  (we use  $N_{\max}^f = 300$ ) for each neural network that has passed the selection described above. Further the mean value of the predictions of the observable obtained with different oscillator parameters  $\hbar\Omega$  is found in the model space  $N_{\max}^f$ . The  $\bar{E}$ , or  $\bar{r}_m$ , or  $\bar{r}_n$ , or  $\bar{r}_p$  values obtained in this manner are subjected to statistical processing.

Unlike [19], we use the method [24] for statistical processing of neural network predictions that have passed the selection, which allows one to take into

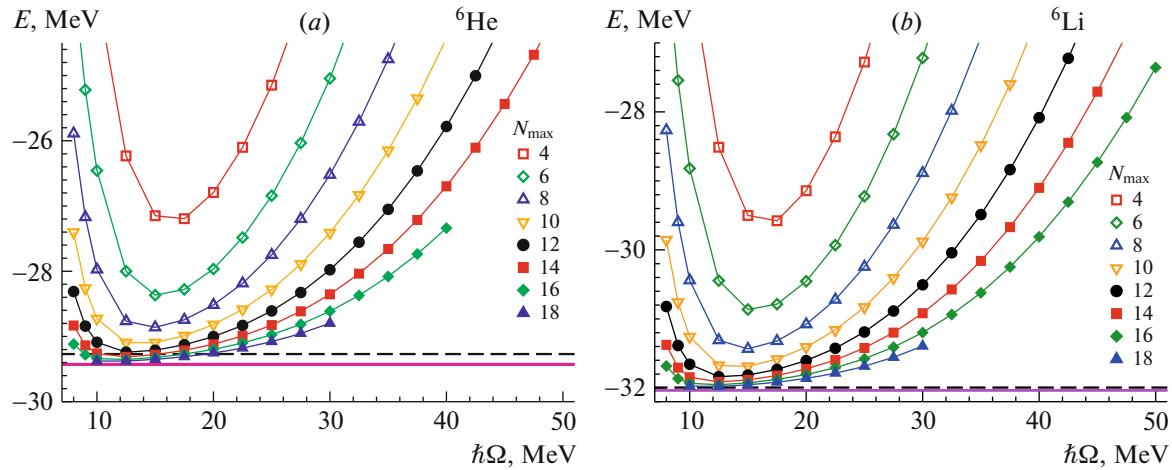


**Fig. 2.** Energies of the ground states of  ${}^6\text{He}$  (a) and  ${}^6\text{Li}$  (b) nuclei calculated within NCSM with the  $NN$  interaction Daejeon16. Dashed lines are experimental values [23]; solid horizontal lines are our extrapolation results (the error in energy predictions is of the order of 10 keV and does not exceed the line thickness).

account more correctly the deviation of the results from the normal distribution, including the asymmetry of the distribution. The essence of this method is that the distribution of results on their magnitude is divided into four areas, each of which contains 25% of the results. The boundaries of these areas are shown by dashed vertical lines in Fig. 4a, where as an example, the distribution of energy predictions for the ground state of the  ${}^6\text{He}$  nucleus is given with a training set from model spaces up to  $N_{\max}^u = 12$ .

The dotted line in the center, the median, divides the distribution into two parts equal in the number of results and does not coincide with the mean value in the case of an asymmetric distribution [24]. The energy value corresponding to the median is denoted by  $\bar{E}^{(1)}$ . The left-hand dashed line, located at a distance of  $\Delta E_1^{(1)}$  from the median, cuts off 25% of the results with the lowest energies, and the right-hand one, located at a distance of  $\Delta E_2^{(1)}$  from the median, cuts off 25% of the results with the highest energies obtained in the selected networks. The energy interval between the dashed lines is denoted by  $\Delta E^{(1)} = \Delta E_1^{(1)} + \Delta E_2^{(1)}$ . Owing to the asymmetry of the distribution,  $\Delta E_1^{(1)} \neq \Delta E_2^{(1)}$ .

Next, the obvious outliers of the results are filtered out according to their magnitude. The filtering method is quite simple [24]: before the final statistical processing, all results to the left of the energy value  $\bar{E}^{(1)} - \Delta E_1^{(1)} - 1.5\Delta E^{(1)}$  and to the right of the energy value  $\bar{E}^{(1)} + \Delta E_2^{(1)} + 1.5\Delta E^{(1)}$  are discarded; the filtering boundaries are indicated in Fig. 4a by solid vertical lines. Typically, the number of outliers (in this figure, the outliers are mainly to the left of

the left-hand filtering boundary) is small and ranges from 10 to 40 selected networks. Thus, the filtering procedure allows one to refine the predictions of the observables, while hardly reducing their statistical reliability.

The median  $\bar{E}$  and scatter  $\Delta E = \Delta E_1 + \Delta E_2$  are then calculated from the filtered sample, which are taken as our prediction and its uncertainty, obtained using the neural networks that have passed the selection. We present the final result as  $E = \bar{E}^{+\Delta E_2}_{-\Delta E_1}$  with asymmetric errors, since, generally speaking,  $\Delta E_1 \neq \Delta E_2$ . The uncertainty of predictions indirectly characterizes the uncertainty in the trained parameters of the machine learning model.

Statistical processing of results for rms radii is carried out in a similar way.

Note that the final number of selected trained networks after filtering depends on the specific problem, but, as a rule, exceeds half of the original ensemble (more than 500). Thus, the statistical reliability of our predictions is higher than in [14], where the final predictions are made on the basis of 50 selected networks.

## 5. EXTRAPOLATION RESULTS

The extrapolation results for the ground state energy of  ${}^6\text{He}$  and  ${}^6\text{Li}$  nuclei obtained using an ensemble of 1024 neural networks are shown in Figs. 5a and 5b. The training sets include NCSM calculations in the range of  $\hbar\Omega$  values from the local minimum in the  $\hbar\Omega$  dependence of  $E(\hbar\Omega)$  to  $\hbar\Omega = 40$  MeV in model spaces  $N_{\max}$  from  $N_{\max}^l = 4$  to  $N_{\max}^u$  (the  $N_{\max}^u$  values are plotted along the horizontal axis). In

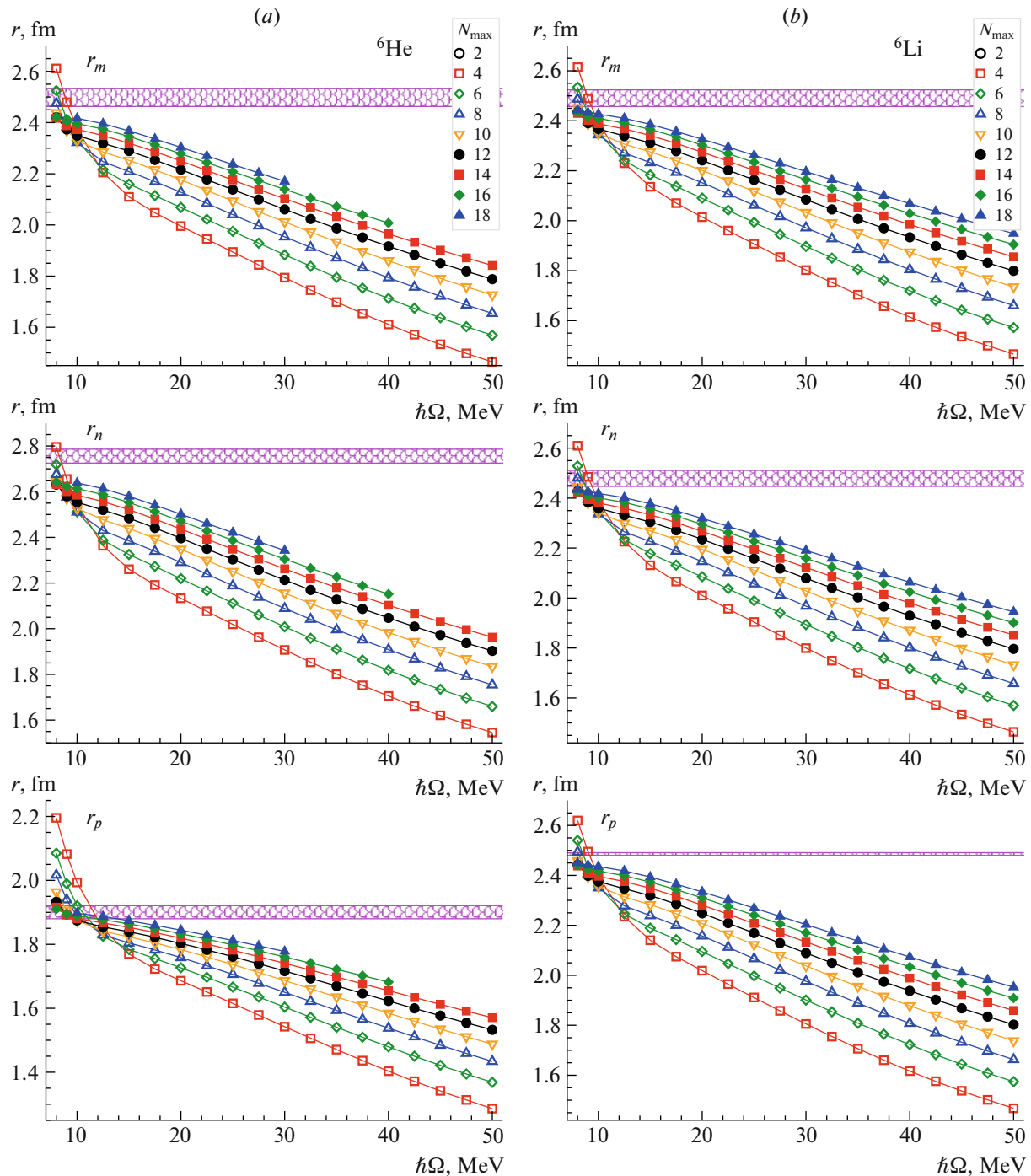


**Fig. 3.** NCSM calculations with the  $NN$  interaction Daejeon16 of rms point radii  $r_m$ ,  $r_n$ , and  $r_p$  in the ground states of  ${}^6\text{He}$  (a) and  ${}^6\text{Li}$  (b) nuclei. The horizontal shaded areas are our extrapolation results together with their uncertainties. The labeling of the model spaces is as in Fig. 2.

the same figure, for comparison, the energies corresponding to the minima of variational calculations in model spaces with  $N_{\text{max}} = N_{\text{max}}^u$ , as well as energies obtained by simple phenomenological extrapolation B [5], are presented.

The energy predictions for both nuclei show good convergence. The uncertainty of the results decreases

with  $N_{\text{max}}^u$  and for maximum values of  $N_{\text{max}}^u = 18$  is less than 7 keV for the  ${}^6\text{He}$  nucleus and less than 3 keV for the  ${}^6\text{Li}$  nucleus, which is comparable with the accuracy of NCSM calculations, which is 1 keV, and does not exceed the extrapolation uncertainty for the  ${}^6\text{Li}$  nucleus in [14].

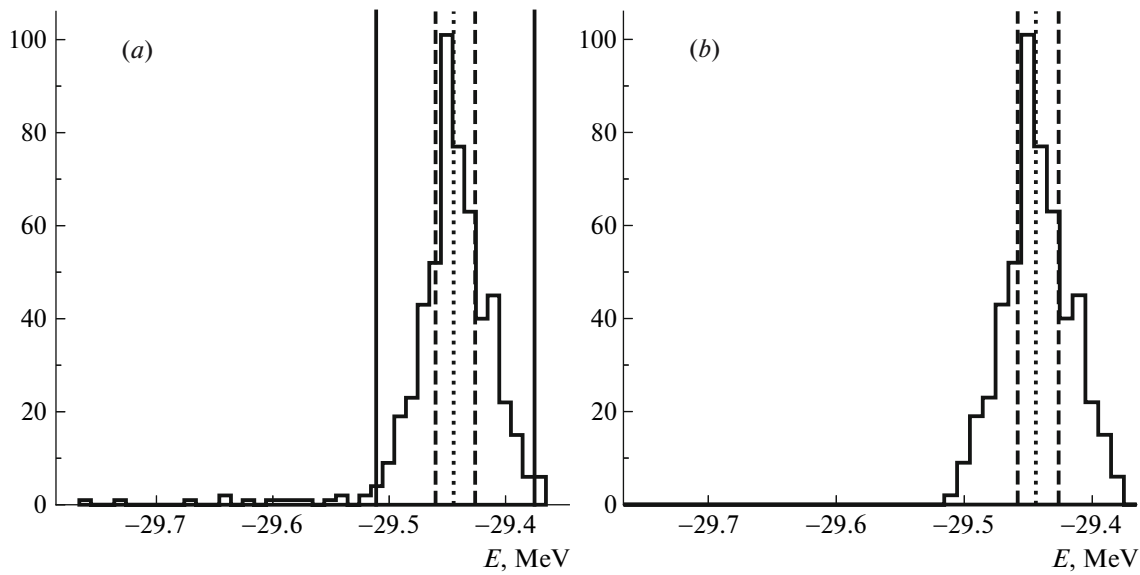


**Fig. 4.** Distribution of ground state energy predictions before (a) and after (b) outlier filtering. The number of neural networks is plotted vertically. The dotted lines show the medians, and the dashed lines show the boundaries corresponding to the interval  $\Delta E^{(1)} = \Delta E_1^{(1)} + \Delta E_2^{(1)}$  before filtering (a) and uncertainties  $\Delta E = \Delta E_1 + \Delta E_2$  (b). The solid lines in panel (a) show the filtration boundaries.

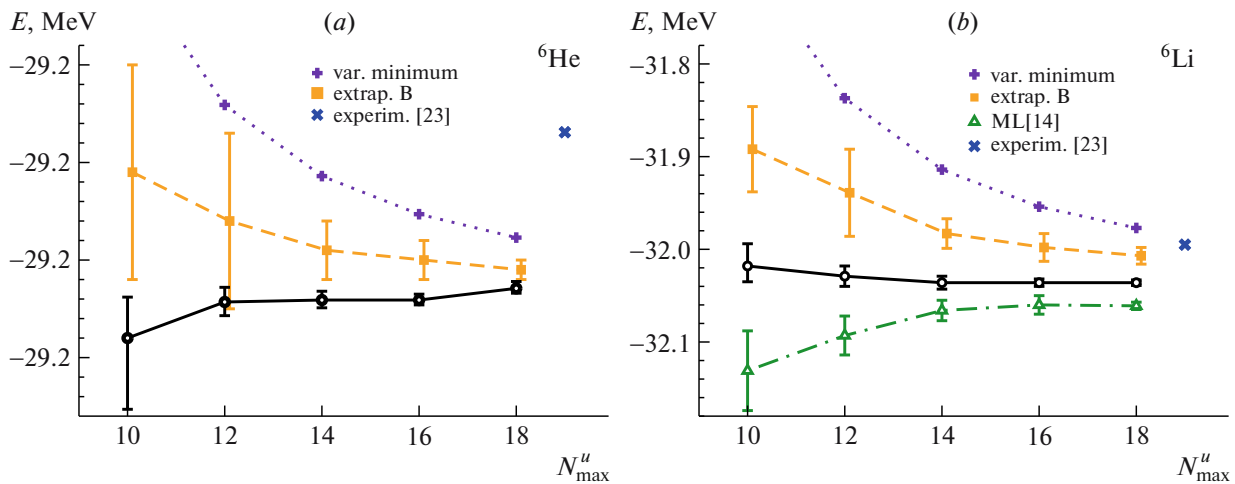


**Fig. 5.** Convergence of the ground state energy predictions of (a)  ${}^6\text{He}$  and (b)  ${}^6\text{Li}$  nuclei as the training data increases by including of the model spaces up to  $N_{\text{max}}^u$ . Empty circles are our calculations, pluses are the variational minimum of calculations in NCSM, solid squares are extrapolation B results, and triangles are the results of extrapolation based on machine learning in [14]. Oblique crosses correspond to the experimental energies of the ground states of  ${}^6\text{He}$  ( $E_{\text{gs}} = -29.269$  MeV) and  ${}^6\text{Li}$  ( $E_{\text{gs}} = -31.995$  MeV) nuclei [23].

The  ${}^6\text{Li}$  nucleus is of particular interest to us, since the extrapolation of the energy and the rms radius of the distribution of point protons  $r_p$  in this nucleus was studied using machine learning methods in the pioneering work [14]. Moreover, the authors of [14] and we use training sets based on the results of NCSM calculations with the same  $NN$  interaction Daejeon16. However, the topology of the neural network, the selection of input data (e.g., we did not divide them into training and test sets), and indi-

vidual aspects of the machine learning extrapolation methodology differ. The differences between the two approaches are described in detail in [19].

Our predictions are below the results of extrapolation B for the  ${}^6\text{Li}$  nucleus, but above the extrapolation results using machine learning in [14]. The uncertainties of these methods in calculations with the same  $N_{\text{max}}^u$  do not overlap. Thus, approaches based on neural network training methods—ours and the one presented in [14]—lead to different predic-

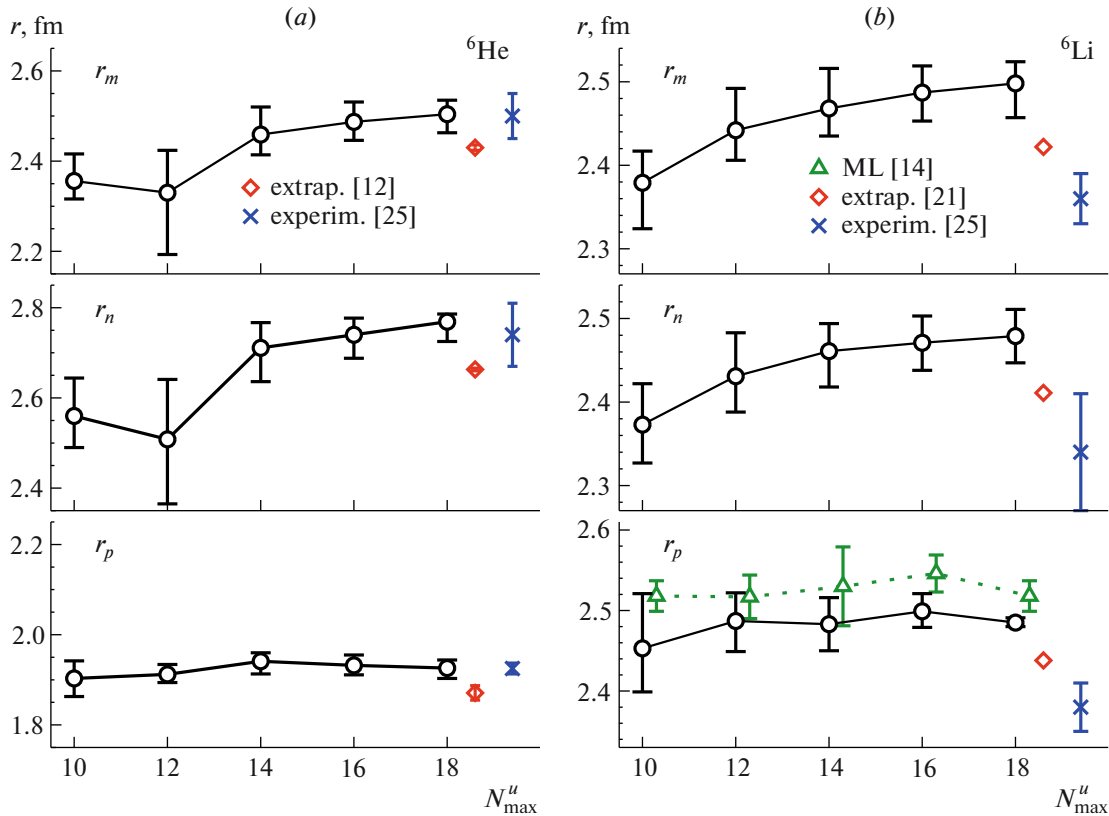


**Fig. 6.** Convergence of neural networks predictions for the rms radii  $r_m$ ,  $r_n$ , and  $r_p$  of the ground states of  ${}^6\text{He}$  (a) and  ${}^6\text{Li}$  (b) nuclei with increasing  $N_{\text{max}}^u$ . Empty circles are our calculations; experimental values (oblique crosses) with error bars are taken from [25]. Empty diamonds are the results of phenomenological two-dimensional exponential extrapolation for  ${}^6\text{He}$  [12] and  ${}^6\text{Li}$  [21] nuclei. Empty triangles are the rms radius  $r_p$  for the  ${}^6\text{Li}$  nucleus based on machine learning from [14].

tions. However, we emphasize that because of the use of a larger ensemble of trained neural networks and more precise selection criteria, our results have higher statistical reliability and demonstrate a weaker dependence on  $N_{\text{max}}^u$ .

Figures 6a and 6b shows convergence of extrapolated rms radii  $r_m$ ,  $r_n$ , and  $r_p$  of the ground states of  ${}^6\text{He}$  and  ${}^6\text{Li}$  nuclei with increasing  $N_{\text{max}}^u$ . The relative uncertainty of predictions of the rms radii  $r_n$  and  $r_m$  in calculations with  $N_{\text{max}}^u = 18$  are larger than the relative uncertainties of energies. The relative uncertainty of energy predictions  $\varepsilon_E \sim 0.01\%$  for the  ${}^6\text{Li}$ , while uncertainties  $\varepsilon_n, \varepsilon_m \sim 1.3\%$  for rms radii  $r_n$  and  $r_m$ . We note, however, that the relative prediction uncertainty  $r_p$  is noticeably smaller:  $\varepsilon_p \sim 0.2\%$ . For the  ${}^6\text{He}$  nucleus, the relative uncertainties are  $\varepsilon_E \sim 0.02\%$ ,  $\varepsilon_n, \varepsilon_m \sim 1.4\%$ , and  $\varepsilon_p \sim 1\%$ . In a number of cases, the asymmetry of the distribution of predictions of the selected networks ( $\Delta E_1 \neq \Delta E_2$ ) is clearly evident. Nevertheless, the overall convergence is quite good. We note that the results of predictions for the point-proton rms radius  $r_p$  of the  ${}^6\text{He}$  nucleus are the most stable ones starting from  $N_{\text{max}}^u = 12$ . The

convergence of the predictions of the rms radii  $r_n$  and  $r_m$  for the  ${}^6\text{He}$  nucleus is somewhat worse, as well as the convergence of the predictions of  $r_n$  and  $r_m$  in the ground state of the  ${}^6\text{Li}$  nucleus.

The extrapolation results for rms radii obtained using neural networks coincide within the uncertainties with the experimental data [25] for the  ${}^6\text{He}$  nucleus, but for the  ${}^6\text{Li}$  nucleus they are somewhat higher. Our predictions are generally close to the results of the two-dimensional phenomenological exponential extrapolation of the radii of  ${}^6\text{He}$  [12] and  ${}^6\text{Li}$  [21] nuclei also obtained on the basis of NCSM calculations with  $NN$  interaction Daejeon16. However, in the case of the  ${}^6\text{He}$  nucleus, the results of [12] are lower than both ours and experimental data, while for the  ${}^6\text{Li}$  nucleus, the results of [21] are between ours and experimental values. The predictions of the rms radius  $r_p$  for the  ${}^6\text{Li}$  nucleus obtained by machine learning methods with different  $N_{\text{max}}^u$  in [14], are above ours and above the experimental value [25].

The region of intersection of the  $\hbar\Omega$  dependences  $r(\hbar\Omega)$  obtained in different model spaces is often used to estimate the radius on the basis of NCSM

calculations and its uncertainty [20]. It can be seen from Figs. 3a and 3b that these regions are localized at  $\hbar\Omega \sim 10$  MeV. The same figure shows the results of our predictions together with uncertainties. In all cases, except for the point proton radius of the  ${}^6\text{He}$  nucleus, the extrapolation results are slightly above the regions of intersection of the dependences  $r(\hbar\Omega)$ .

## 6. CONCLUSIONS

Using the machine learning method of the neural networks ensemble proposed in [14] and modified in [19], an extrapolation has been carried out to the case of the infinite basis of the energies  $E$  and distributions of rms radii of point protons  $r_p$ , point neutrons  $r_n$ , and point nucleons (matter)  $r_m$  in the ground states of  ${}^6\text{Li}$  and  ${}^6\text{He}$  nuclei. Neural networks have been trained on training datasets  $N_{\max}$ ,  $\hbar\Omega$ , and  $E$  (or  $r_p$ , or  $r_n$ , or  $r_m$ ), calculated in NCSM with the  $NN$  interaction Daejeon16 in model spaces up to  $N_{\max} = 18$ .

The predictions of the ground state energies of  ${}^6\text{Li}$  and  ${}^6\text{He}$  nuclei show good convergence and in calculations with the largest training data set ( $N_{\max}^u = 18$ ) are  $\bar{E}({}^6\text{Li}) = -32.036 \pm 0.003$  MeV and  $\bar{E}({}^6\text{He}) = -29.429_{-0.005}^{+0.007}$  MeV. The prediction uncertainties are comparable with the accuracy of NCSM calculations (1 keV) and do not exceed the uncertainties of extrapolations based on machine learning in [14], but our results for all  $N_{\max}^u$  values lie higher and the uncertainties of two machine learning extrapolations do not overlap. Thus, the use of different extrapolation methods based on machine learning methods can lead to different results. It is important to emphasize that because of the larger number of trained neural networks that passed the selection, the statistical reliability of our predictions is higher than in [14].

The uncertainty of the predictions of the rms point radii  $r_p$ ,  $r_n$ , and  $r_m$  is slightly worse—about one percent, but, in general, the convergence of the results is also quite good. Our results for the radii are close to the experimental data [25] for the  ${}^6\text{He}$  nucleus and are slightly larger than the experimental values for the  ${}^6\text{Li}$  nucleus. The obtained predictions are generally consistent with the results of the two-dimensional phenomenological exponential extrapolation of the rms point radii of the  ${}^6\text{He}$  [12] and  ${}^6\text{Li}$  [21] nuclei based on the NCSM results with the same  $NN$  interaction Daejeon16. The prediction of the rms radius  $r_p$  obtained by machine learning in [14] suggests larger value than ours and the experimental one.

The considered method for extrapolation is universal and can be applied to other observables, such as the quadrupole moment and the probabilities of electromagnetic transitions in nuclei.

## FUNDING

This work was supported by the Russian Science Foundation, project no. 24-22-00276.

## CONFLICT OF INTEREST

The authors of this work declare that they have no conflicts of interest.

## REFERENCES

1. A. Boehnlein, M. Diefenthaler, N. Sato, M. Schram, V. Ziegler, C. Fanelli, M. Hjorth-Jensen, T. Horn, M. P. Kuchera, D. Lee, W. Nazarewicz, P. Ostroumov, K. Orginos, A. Poon, X.-N. Wang, A. Scheinker, M. S. Smith, and L.-G. Pang, *Rev. Mod. Phys.* **94**, 31003 (2022).  
<https://doi.org/10.1103/revmodphys.94.031003>
2. B. R. Barrett, P. Navrátil, and J. P. Vary, *Prog. Part. Nucl. Phys.* **69**, 131 (2013).  
<https://doi.org/10.1016/j.pnpnp.2012.10.003>
3. R. Machleidt, *Int. J. Mod. Phys. E* **26**, 1730005 (2017).  
<https://doi.org/10.1142/s0218301317300053>
4. H. Zhan, A. Nogga, B. R. Barrett, J. P. Vary, and P. Navrátil, *Phys Rev. C* **69**, 34302 (2004).  
<https://doi.org/10.1103/physrevc.69.034302>
5. P. Maris, J. P. Vary, and A. M. Shirokov, *Phys Rev. C* **79**, 14308 (2009).  
<https://doi.org/10.1103/physrevc.79.014308>
6. S. A. Coon, M. I. Avetian, M. K. G. Kruse, U. Van Kolck, P. Maris, and J. P. Vary, *Phys Rev. C* **86**, 54002 (2012).  
<https://doi.org/10.1103/physrevc.86.054002>
7. P. Maris and J. P. Vary, *Int. J. Mod. Phys. E* **22**, 1330016 (2013).  
<https://doi.org/10.1142/s0218301313300166>
8. M. K. G. Kruse, E. D. Jurgenson, P. Navrátil, B. R. Barrett, and W. E. Ormand, *Phys Rev. C* **87**, 44301 (2013).  
<https://doi.org/10.1103/physrevc.87.044301>
9. S. N. More, A. Ekström, R. J. Furnstahl, G. Hagen, and T. Papenbrock, *Phys Rev. C* **87**, 44326 (2013).  
<https://doi.org/10.1103/physrevc.87.044326>
10. R. J. Furnstahl, S. N. More, and T. Papenbrock, *Phys Rev. C* **89**, 44301 (2014).  
<https://doi.org/10.1103/physrevc.89.044301>
11. I. J. Shin, Yo. Kim, P. Maris, J. P. Vary, Ch. Forssén, J. Rotureau, and N. Michel, *J. Phys. G: Nucl. Part. Phys.* **44**, 075103 (2017).  
<https://doi.org/10.1088/1361-6471/aa6cb7>
12. D. M. Rodkin and Yu. M. Tchuvil'sky, *Phys Rev. C* **106**, 34305 (2022).  
<https://doi.org/10.1103/physrevc.106.034305>
13. A. M. Shirokov, A. I. Mazur, and V. A. Kulikov, *Phys. At. Nucl.* **84**, 131 (2021).  
<https://doi.org/10.1134/s1063778821020149>

14. G. A. Negroita, J. P. Vary, G. R. Luecke, P. Maris, A. M. Shirokov, I. J. Shin, Yo. Kim, E. G. Ng, Ch. Yang, M. Lockner, and G. M. Prabhu, *Phys Rev. C* **99**, 54308 (2019).  
<https://doi.org/10.1103/physrevc.99.054308>
15. W. G. Jiang, G. Hagen, and T. Papenbrock, *Phys Rev. C* **100**, 54326 (2019).  
<https://doi.org/10.1103/physrevc.100.054326>
16. I. Vidaña, *Nucl. Phys. A* **1032**, 122625 (2023).  
<https://doi.org/10.1016/j.nuclphysa.2023.122625>
17. T. Wolfgruber, M. Knöll, and R. Roth, *Phys Rev. C* **110**, 14327 (2024).  
<https://doi.org/10.1103/physrevc.110.014327>
18. M. Knöll, T. Wolfgruber, M. L. Agel, C. Wenz, and R. Roth, *Phys. Lett. B* **839**, 137781 (2023).  
<https://doi.org/10.1016/j.physletb.2023.137781>
19. A. I. Mazur, R. E. Sharypov, and A. M. Shirokov, *Moscow Univ. Phys. Bull.* **79**, 318 (2024).  
<https://doi.org/10.3103/s0027134924700395>
20. A. M. Shirokov, I. J. Shin, Y. Kim, M. Sosonkina, P. Maris, and J. P. Vary, *Phys. Lett. B* **761**, 87 (2016).  
<https://doi.org/10.1016/j.physletb.2016.08.006>
21. D. M. Rodkin and Yu. M. Tchuvil'sky, *JETP Lett.* **118**, 153 (2023).  
<https://doi.org/10.1134/s0021364023602130>
22. D. P. Kingma and J. Ba, arXiv:1412.6980 (2014).  
<https://doi.org/10.48550/arXiv.1412.6980>
23. D. R. Tilley, C. M. Cheves, J. L. Godwin, G. M. Hale, H. M. Hofmann, J. H. Kelley, C. G. Sheu, and H. R. Weller, *Nucl. Phys. A* **708**, 3 (2002).  
[https://doi.org/10.1016/s0375-9474\(02\)00597-3](https://doi.org/10.1016/s0375-9474(02)00597-3)
24. R. R. Wilcox, *Basic Statistics: Understanding Conventional Methods and Modern Insights* (Oxford University Press, New York, 2009). <https://doi.org/10.1093/oso/9780195315103.001.0001>
25. I. Tanihata, H. Savajols, and R. Kanungo, *Prog. Part. Nucl. Phys.* **68**, 215 (2013).  
<https://doi.org/10.1016/j.pnpnp.2012.07.001>

*Translated by L. Mosina*

**Publisher's Note.** Pleiades Publishing remains neutral with regard to jurisdictional claims in published maps and institutional affiliations.

AI tools may have been used in the translation or editing of this article.